

**Interdecadal changes in the ENSO teleconnection to the  
Caribbean region and the North Atlantic Oscillation.** <sup>1</sup>

Alessandra Giannini, Mark A. Cane and Yochanan Kushnir

*Lamont-Doherty Earth Obs. of Columbia University*

*Palisades, NY 10964*

*Journal of Climate, in press*

4 Jan 2001

<sup>1</sup>Contribution number 6148 of Lamont Doherty Earth Observatory.

## **Abstract**

The El Niño-Southern Oscillation (ENSO) phenomenon and variability in subtropical North Atlantic High sea level pressure (SLP) are known to affect rainfall in the Caribbean region. An El Niño event is associated with drier than average conditions during the boreal summer of year (0), and wetter than average conditions during the spring of year (+1). Dry conditions during the summer of year (0) of an El Niño are associated with the locally divergent surface circulation engendered by the eastward shift of deep convection in the Pacific Ocean. Wet conditions during the spring of year (+1) of an El Niño are associated with the lagged warming of the tropical North Atlantic Ocean. Variability in the strength of the North Atlantic High is governed mainly by the North Atlantic Oscillation (NAO) with a positive NAO phase implying a stronger than normal High and viceversa. The NAO is negatively correlated with Caribbean rainfall, indirectly, via anomalous sea surface temperatures (SST) associated with anomalies in the surface wind speed at tropical latitudes, and directly, via anomalous subsidence. The combined effect of the two phenomena is found to be strongest when the two signals interfere constructively:

- during the summer following winters characterized by the positive phase of the NAO, the dryness associated with a developing warm ENSO event adds to the dryness associated with a positive SLP anomaly in the subtropical North Atlantic (7 out of 11 El Niños between 1949 and 1999 fall in this category);
- during the spring following winters characterized by the negative phase of the NAO, the wetness that follows a warm ENSO event is augmented by the wetness associated with the warmer than average tropical North Atlantic SSTs (5 out of 11 El Niños between 1949 and 1999 fall in this category).

The coincidence in the recurrence of a positive phase of the NAO during the winters coinciding with peak warm ENSO conditions has increased in the last 20 years compared to the previous few decades. This partially explains the noticeable consistent dry signal over the Caribbean during the summer of year (0) of a warm ENSO event, and the disappearance of the wet signal during the spring of year (+1) in the recent record.

## 1. Introduction

The Caribbean basin, the 'warm pool' of the tropical North Atlantic, is known to be affected by climate variability of Atlantic and Pacific origin. Both ENSO and the North Atlantic subtropical High SLP center (hereafter referred to as NAH) independently modulate rainfall in the Caribbean/Central American region on an interannual timescale (Hastenrath 1976, 1984; Ropelewski and Halpert 1987, 1996; Kiladis and Diaz 1989; Enfield 1996; Enfield and Alfaro 1999; Giannini et al. 2000, hereafter referred to as GKC). The variability associated with the large-scale circulation can be distinguished from small-scale, localized effects, such as topography, and accounts for 10 to 20% of the total seasonal variance, depending on season considered.

Most of the Caribbean region shares a characteristic double-peaked rainy season, with maxima in spring (May-June) and fall (September-October), an absolute minimum during the winter dry season (January-March), and a relative minimum at the peak of summer (July-August) (GKC). With respect to the annual cycle, the high internal variability of the wintertime atmosphere in the North Atlantic sector is reflected best in Caribbean rainfall variability during spring, at the start of the rainy season. A stronger than average NAH during winter, associated with the positive phase of the NAO (van Loon and Rogers 1978), translates into stronger trade winds on its equatorward flank and enhanced heat loss from the ocean into the atmosphere (Cayan 1992; Seager et al. 2000). The cooling of the tropical ocean attains maximum spatial coherence in spring, when it is associated with weakened convection in the Caribbean, before slowly decaying under the damping effect of local thermodynamic processes. The effect on spring rainfall is particularly evident for the stations on the Antilles islands. Figure 1 shows the correlation of the

December-to-March NAO index (Hurrell 1995)<sup>1</sup> with spring station rainfall. Only those stations that have at least 66% of the data, i.e. 20 of 30 years during 1949-1980, are retained and among them only the ones that reach the 95% significance level for correlation (0.425 for 20 degrees of freedom; Snedecor and Cochran 1989) are plotted. Wintertime NAH also shows a weak positive correlation with SLP over the Central American monsoon region during the following summer (Hastenrath 1976). To explain the persistence of SST anomalies generated in winter beyond a damping timescale of a few months, it is reasonable to invoke a positive feedback, e.g. between SST and cloud cover. Enhanced low-level cloud cover over cooler SST would prolong the lifetime of the SST anomalies, allowing them to still affect the summertime atmosphere (Knaff 1997). The mid-summer dry spell characteristic of many stations throughout the region is enhanced following a positive NAO winter.

The typical signature of ENSO events<sup>2</sup> in the Caribbean/Central American region is a reversal in the sign of the correlation of the Niño-3 index with rainfall between the year of ENSO onset (hereafter year (0)) and the following year (year (+1)). To depict this reversal we choose seasons in a way that compromises between the pattern of the local annual cycle in rainfall (i.e. the peaks in spring and fall, and the mid-summer break) and the lifecycle of an ENSO event. Fig. 2 shows the correlation of peak Niño-3 with rainfall during the summer of year (0) (July to September, or JAS(0)), and during the spring of year (+1) (April to June, or AMJ(+1)). The December(0)-January(+1) Niño-3 (Kaplan et al. 1997, 1998) was used to identify the events over

---

<sup>1</sup>Available from [http://www.cgd.ucar.edu/cas/climind/nao\\_winter.html](http://www.cgd.ucar.edu/cas/climind/nao_winter.html).

<sup>2</sup>We refer to 'El Niño' and 'warm ENSO event' as synonyms, describing the warm phase of ENSO. Following Rasmusson and Carpenter (1982), we label with a '(0)' the seasons in the year of onset of the ENSO event, which occurs during (boreal) spring. The '(+1)' label refers to the following year, the one that witnesses the decay phase in spring.

the interval 1949-1980. The same statistical considerations made for fig. 1 apply here. Rainfall correlations are negative during the summer of year (0) prior to the peak phase of El Niño, and positive after it. In fact, the reversal of the negative signal starts at the northwestern corner of the basin (Yucatan and Cuba, the region directly affected by extratropical fronts (Schultz et al. 1998)) during the winter coinciding with the peak of ENSO, and spreads to the Antilles in spring of year (+1).

The ENSO teleconnection to the Atlantic sector is part of the 'atmospheric bridge' described by Lau and Nath (1994; 1996; Lau 1997) and can be decomposed into a tropical and an extratropical component (GKC; see their figure 4). The tropical response is solely dependent on the presence of anomalous heating in the central and eastern equatorial Pacific. It manifests itself as a zonal seesaw in SLP: when SLP is lower than average over the warmer tropical Pacific waters, it is higher than average over the tropical Atlantic (Hastenrath and Heller 1977; Covey and Hastenrath 1978; Curtis and Hastenrath 1995; Poveda and Mesa 1997). The trade winds weaken in the Atlantic, consistent with the diminished meridional SLP gradient in this sector. The zonal seesaw in SLP results in surface convergence to the southwest of the Caribbean basin, onto the eastern Pacific ITCZ, and in divergence in the basin, hence the drier than average conditions during July to October of year (0) (Ropelewski and Halpert 1987, 1996). The extratropical response to ENSO, confined to the winter season, takes on the form of the Pacific-North American (PNA) teleconnection pattern (Horel and Wallace 1981; Wallace and Gutzler 1981; Barnston and Livezey 1987; Trenberth et al. 1998), an equivalent barotropic pattern with centers of action of opposite sign over the North Pacific, northern North America, and the southeastern U.S. and Gulf of Mexico. The last center of action in the PNA wave train, the lower than average SLP

over Florida and the subtropical western Atlantic, further contributes to the weakening of the meridional SLP gradient, and of the trades. Thus, following a warm ENSO event, evaporation in the tropical North Atlantic is diminished, and the delayed warming that ensues (Pan and Oort 1983; Nobre and Shukla 1996; Enfield and Mayer 1997; GKC) increases Caribbean convection and rainfall in a way very similar to that ascribed to a negative NAO phase. Note that following a warm ENSO event the tropical North Atlantic warms and the Caribbean experiences wetter conditions, simultaneously with the drier conditions in Northeast Brazil. This coincidence may be ascribed to variability in the meridional positioning of the Atlantic ITCZ, with the remote effect of ENSO playing a major role (Chiang et al. 2000).

In this study, we seek to extend to the more recent two decades the conclusions of our previous research (GKC) on the respective roles of ENSO and the NAO in Caribbean rainfall variability. For this purpose, we analyze two independent rainfall datasets, the station records previously used, covering 1949 to 1980, and a merged analysis of satellite-retrieved and rain-gauge data (Xie and Arkin 1996, 1997), covering 1979 to present. The advantage in using the latter data comes from its global extent. In particular, its coverage of the tropical oceans allows the explicit depiction of the global ENSO teleconnection pattern. The most glaring disadvantage comes from the short length of the time series. A preliminary comparison of these independent rainfall datasets reveals significant differences in the ENSO teleconnection to Caribbean/Central American rainfall. Since both GKC and Enfield and Alfaro (1999) highlight the complementary roles of the tropical Pacific and North Atlantic on Caribbean/Central American climate, we focus our investigation on the ENSO-NAO interaction. However, other sources of interdecadal variability briefly discussed in the final section of the paper should not be discounted. Most

notably, warm ENSO events have displayed unusual character since the mid 1970s.

Enfield and collaborators (Enfield 1996; Enfield and Alfaro 1999) focus on Atlantic and Pacific patterns of SST variability associated with rainfall anomalies in the Caribbean and Central America. They find, for example, that rainfall is enhanced in the presence of an interbasin gradient in SST anomalies, when the tropical North Atlantic is warmer than average and the eastern equatorial Pacific is cooler than average<sup>3</sup>. In our study we present a coherent picture of the oceanic and atmospheric anomalies affecting the Caribbean/Central American region. The connection of the SST anomalies of Enfield and Alfaro (1999) to their atmospheric sources, the ENSO teleconnection and the impact of the NAO on the tropical North Atlantic, further enhances the prospects for predictability of rainfall anomalies.

The data used is described in section 2. In section 3 we compare the ENSO teleconnection to the Caribbean basin in the two independent rainfall datasets covering non-overlapping periods. In section 4 we present an explanation for the differences in the comparison presented in section 3. To clarify the nature of the interaction between the NAO and ENSO, in section 5 we focus on winter, when the fingerprint of both signals over the North Atlantic is clearest. A summary and final considerations are drawn in section 6.

---

<sup>3</sup>On the basis of the recurrence of such conditions following the major ENSO event of 1997-98, the Center for Geophysical Investigations at the University of Costa Rica (Centro de Investigaciones Geofisicas de la Universidad de Costa Rica) issued 'a successful climate outlook in early March 1999 for the 1999 rainy season (May-November) in lower Central America' (Alfaro and Enfield 1999). The outlook called for an early onset of the rains.

## 2. Data

A central problem in the assessment of the interdecadal variability of rainfall is the spatio-temporal discontinuity in the datasets. The limited spatial coverage of land station records is in contrast with the global satellite coverage achieved during the last 20 years. In GKC, we made use of the individual station data extracted from the National Oceanic and Atmospheric Administration (NOAA) National Climatic Data Center (NCDC) Global Historical Climatological Network (GHCN)) (Vose et al. 1992, hereafter referred to as station data, or GHCN). We selected stations from the Caribbean/Central American region, which we define to be  $5^{\circ}\text{N}$  to  $25^{\circ}\text{N}$ , and  $90^{\circ}\text{W}$  to  $60^{\circ}\text{W}$ . In the tropics, GHCN records typically yield satisfactory coverage during the years 1950-80, studied in GKC, with a few records extending back into the early part of the twentieth century. Fig. 3 shows the sharp decline in the number of weather stations in the Caribbean/Central American region reporting in the last 20 years.

In the present study we focus on the 1949-1999 period covered by the NCEP-NCAR reanalysis project (Kalnay et al. 1996), complementing the analysis of rainfall variability with that of surface data (mean sea level pressure, surface temperature<sup>4</sup>). Due to the decline in the number of stations since 1980, the spatial coverage necessary to connect the regional aspects of rainfall variability to the large-scale patterns of ocean-atmosphere interaction is sufficient only in the earlier part of the NCEP Reanalysis, from 1949 to 1980. In the latter part of the record (1979-1999), we use the NOAA National Centers for Environmental Prediction (NCEP) Climate

---

<sup>4</sup>Mean sea level pressure is a type-A variable in the classification given by Kalnay et al. (1996), i.e. 'it is strongly influenced by observed data, and hence it is in the most reliable class', whereas surface temperature is a type-B variable, i.e. 'although there are observational data that directly affects the value of the variable, the model also has a very strong influence on the analysis value'.



Prediction Center (CPC) Merged analysis of rainfall (Xie and Arkin 1996, 1997; hereafter referred to as Xie-Arkin), a dataset obtained by merging available rain gauge measurements with satellite observations, to characterize the spatial patterns of the ENSO teleconnection to the Caribbean.

To partially justify this approach, Fig. 4 compares two indices of rainfall, one from Xie-Arkin and the other from GHCN. The GHCN index is constructed by averaging rainfall at 9 Caribbean stations whose records extend to 1999. The 9 stations are all located on the Antilles Islands<sup>5</sup>. The Xie-Arkin index is an average of the gridded data in the region bounded by 15°N and 22.5°N, 80°W and 60°W, covering the Antilles. The two indices are compared separately for the summer and spring seasons (fig. 4, left and right, respectively). The good agreement is in part due to the fact that Xie and Arkin’s algorithm incorporates information from station data. Trends are visible in both indices, over the 1979-1999 period. The negative trends in the spring season (fig. 4, right panel), of the order of 3.4 and 7 mm/year, for Xie-Arkin and GHCN, respectively, are statistically significant at the 95% level. The negative trends in the summer season (fig. 4, left panel), on the other hand, of 1.7 mm/year in Xie-Arkin and 1.3 mm/year in GHCN, are not robust.

### 3. Caribbean rainfall variability over the recent 20 years

The spatially continuous coverage -land and ocean- of the Xie-Arkin data enables us to re-examine the dynamical hypotheses set forth in GKC in a broader sense, and to extend their

---

<sup>5</sup>Two stations, Kingston/Manley International Airport and Cinchona Hill Garden, are in Jamaica, 4, Santo Domingo, Puerto Plata, La Vega and Sanchez, are in the Dominican Republic, 2, San Juan International Airport and Fajardo, are in Puerto Rico and one, Charlotte Amalie, is in the Virgin Islands.

conclusions to the present. We start by comparing the correlation maps of the Niño-3 index with Caribbean rainfall during JAS(0) and AMJ(+1) of 1949-1980 (fig. 2), with composites of rainfall anomalies representative of El Niño and La Niña events for the satellite-derived rainfall measurements (1979-1999) (fig. 5). For this recent period we composite warm and cold ENSO events separately. We use Niño-3 to separate warm, cold and neutral years. When the SST anomaly in the central and eastern equatorial Pacific is 1°C or greater during December(0)-January(+1), i.e. during the mature ENSO phase, the seasons belonging to year (0) and leading to the mature phase, as well as those immediately following it in year (+1), are categorized as 'warm'<sup>6</sup>. If the December-January Niño-3 is less than -0.75°C, the same seasons are categorized as 'cold'<sup>7</sup>. The threshold used to define La Niñas is lower, to reflect the skewness in the distribution of Niño-3 SST anomalies. The remaining 12 years fall into the 'neutral' category.

To allow for its non-normal distribution, rainfall is ranked separately for warm and neutral, or cold and neutral conditions, and a Wilcoxon two-sample sum statistic (Hollander and Wolfe 1999) is applied to the ranks. The ranks of the warm, or cold, years only, respectively, are summed together:

$$W = \sum_{i=1}^n \text{rank}(ENSO_i)$$

and compared with an 'average' rank. The significance in the difference of the rank of warm, or cold, and neutral seasons is assessed, in the limit of large numbers, by estimating the 'average'

---

<sup>6</sup>The years are 1982-83, 1986-87, 1987-88, 1991-92, 1994-95 and 1997-98.

<sup>7</sup>The years are 1984-85, 1988-89 and 1998-99.

mean and variance of  $W$ :

$$E(W) = \frac{n(n + m + 1)}{2}$$

$$var(W) = \frac{mn(n + m + 1)}{12}$$

where  $E$  is the expectance operator. Typically,  $n < m$ , so that  $n$  is the number of warm, or cold, years, and  $m$  is the number of neutral years. The  $W^*$  statistic:

$$W^* = \frac{W - E(W)}{\sqrt{var(W)}}$$

represents the deviation of the rank of the warm, or cold, years from the 'average' rank, in units of standard deviation. Because  $W^*$  is normally distributed, the significance level follows implicitly.

In the rank anomaly composites of warm JAS(0) rainfall, in fig. 5 (top left panel), negative anomalies are apparent over Central America, the Caribbean, and the tropical North Atlantic. Shading indicates one-sided statistical significance at the 95% confidence level. The sign is reversed in the case of cold JAS(0) (fig. 5, bottom left panel). The association between Niño-3 and summer Caribbean rainfall found for the station data is reproduced in the more recent period, and over the adjacent oceanic regions.

The rank anomaly composites of AMJ(+1) tell a different story. In cold ENSO events, anomalies in the Caribbean and tropical North Atlantic switch from positive in JAS(0) to neg-

ative in AMJ(+1). In warm ENSO events, on the other hand, negative anomalies over Central America persist from summer of year (0) to spring of year (+1). These results are only partially consistent with the picture of the ENSO teleconnection to the Caribbean/Central American region established in the literature, e.g. the global surveys of Ropelewski and Halpert (1987, 1996) and Kiladis and Diaz (1989), and the regional studies of Hastenrath (1976, 1984), Waylen et al. (1996), Enfield (1996), Chen et al. (1997), Enfield and Alfaro (1999), and GKC. The JAS(0) anomaly is reproduced in the recent period, but the AMJ(+1) anomaly is only partially so. Figure 5 highlights the question we want to answer: what explains the differences in the ENSO teleconnection to the Caribbean apparent in the period 1979-99?

#### **4. The impact of the trend in the NAO on spring Caribbean rainfall**

Thus far we have considered the impact of ENSO on Caribbean rainfall independent of the state of North Atlantic climate. To explain the observed changes in the ENSO teleconnection during the last 20 years we turn to the relationship between ENSO and the NAO. Given that we know the way in which the two phenomena independently affect Caribbean rainfall we can hypothesize the impact of their mutual relationship. A warm ENSO and a positive NAO should combine their negative impacts on summer rainfall in the Caribbean, since they both affect the local atmospheric circulation in such a way as to favor surface divergence, or subsidence, hence negative rainfall anomalies. A warm ENSO and a negative NAO, both associated with positive SST anomalies in the tropical North Atlantic in spring, should associate with positive rainfall anomalies in the Caribbean.

Figure 6 shows the amplitude of the December-January Niño-3 for all warm and cold

events during the 20<sup>th</sup> century. The height of the bar represents the magnitude of the Pacific SST anomaly during mature conditions, the color represents the magnitude of the NAO. The December(0)-January(+1) Niño-3 is contrasted with the NAO index during December-to-March of year (0) (fig. 6, left panel), and of year (+1) (fig. 6, right panel). The former set of indices is the relevant one for the summer of year (0) (JAS(0)). The SST anomalies have already established themselves in the tropical Pacific, and so has the global anomalous atmospheric circulation that accompanies them, which directly affects the Caribbean. The latter bears a close relationship with rainfall during spring of year (+1) (AMJ(+1)), as the ENSO event is decaying. Then, the delayed SST response in the tropical Atlantic becomes dominant. In both cases we note that the ENSO events of the last 20 years coincide more frequently with the positive phase of the NAO. This should not come as a surprise, given the recent trend in North Atlantic climate.

Composites of surface temperature and mean sea level pressure, this time for the entire 51-year period spanned by the recent extension of the NCEP-NCAR reanalysis, are shown for warm ENSO JAS(0) and AMJ(+1) in figures 7 and 8. Shading represents 95% statistical significance of the difference between warm ENSO and neutral conditions as measured by a standard *t*-test. The warming of the tropical Pacific is already evident during the summer of year (0) (fig. 7, top left). It is accompanied by the seesaw in tropical sea level pressure between the Pacific and Atlantic basins (fig. 7, top right). A weak cooling of the tropical Atlantic, possibly related to the local strengthening of the trade winds, as they accelerate towards the anomalous Pacific heat source, is barely noticeable. When only those warm ENSO events that have been preceded by a positive NAO winter are composited, the signature of the NAO on North Atlantic SST becomes more clearly discernible, with the typical tripole pattern especially emphasized in its

high and low latitude components. 7 out of the 11 warm ENSO events between 1949 and 1999, and 4 out of the 6 events since 1979, fall in this category (fig. 6, left panel). The cooling of the tropical North Atlantic reaches statistical significance, which is augmented by the dynamical significance of the matching SLP pattern. In the Caribbean basin and western tropical North Atlantic the cool SST overlain by the high SLP (fig. 7, bottom panels) is strongly suggestive of a local thermodynamical coupling between the externally forced SSTs and the atmosphere.

In spring (+1) the tropical North Atlantic warms up (Enfield and Mayer 1997) (fig. 8). To show the superposition of the effects of ENSO and the NAO on tropical North Atlantic SST, we divide warm ENSO events according to the phase of the NAO during winter (+1). 5 out of the 11 warm ENSO events between 1949 and 1999, 4 out of 5 before 1979, are contemporary with the negative phase of the NAO during December (0) to March (+1). This is when the two phenomena interfere constructively, and SST anomalies are more coherent spatially. However in the 1949-99 sample the negative NAO phase serendipitously coincides with the weaker warm ENSO events. That is why the warm ENSO-negative NAO anomalies are weaker than the all-warm ENSO anomalies, especially on the western side of the basin (cf. the top and middle panels in fig. 8). The December(0)-January(+1) Niño-3 value is smaller than  $1.5^{\circ}\text{C}$  in all 5 negative NAO cases, while coincident with the positive phase of the NAO in the warm ENSO events of 1972-73, 1982-83 and 1997-98, Niño-3 is equal to or greater than  $2^{\circ}\text{C}$ . Nevertheless, any significance in the SST anomalies between  $5^{\circ}$  and  $25^{\circ}\text{N}$  has disappeared, due to the destructive interference between warm ENSO and positive NAO (fig. 8, bottom panel).

As an attempt to quantify the relative impacts of ENSO and the NAO on tropical North Atlantic SST we regress an average of April-to-June SST in the region between  $5^{\circ}$  and  $25^{\circ}\text{N}$ ,

60° and 15°W (hereafter referred to as tNA) against the December-March NAO and December(0)-January(+1) Niño-3 indices:

$$tNA(t) = a + bNAO(t) + cNINO3(t)$$

Regressions are computed for the period 1900-1991 using the Kaplan et al (1997, 1998) reconstruction of global sea surface temperature<sup>8</sup>, and for the period 1949-1999 and subperiod 1979-1999 using NCEP surface temperature. Table 1 summarizes the results. The NAO and Niño-3 are regressed separately in the first two lines respectively relating to each period and together in the third line. Column 5 is the correlation coefficient ( $r$ ) between regressed and observed tNA, and column 6 is Akaike's information criterion (hereafter referred to as AIC; Akaike 1974; Cook et al. 1996, 1999). AIC balances the cost of adding another variable to the regression with the value of the added information. It is proportional to the variance in the residual between the observed and modeled tNA and to the number of variables considered in the regression. When AIC is decreased by adding another variable to the regression, it means that such a variable adds valuable information to the regression.

Two observations can be made on table 1: (1) Niño-3 explains a greater percentage of the variance of tNA (between 19 and 31%) than does the NAO index (between 5 and 10%); (2) consideration of the NAO index improves the regression in all periods except the most recent one, during which the positive phase of the NAO has persisted.

The imprint of the negative NAO on the ENSO-related warming of the tropical North

---

<sup>8</sup>[http://ingrid.ldeo.columbia.edu/SOURCES/.KAPLAN/.RSA\\_MOHSST5.cuf/.dataset\\_documentation.html](http://ingrid.ldeo.columbia.edu/SOURCES/.KAPLAN/.RSA_MOHSST5.cuf/.dataset_documentation.html).

Atlantic is manifest in the strength of the anomalies off the coast of West Africa in the eastern portion of the basin, consistent with the fact that the sea level pressure pattern associated with the NAO is shifted eastward with respect to the region of maximum wintertime ENSO influence, as will be shown in the next section. Close to the West African coast the weakening of the trade winds associated with the negative phase of the NAO forces a reduction in surface heat fluxes as well as a reduction in coastal upwelling, hence the enhanced warming. The warming of the surface ocean is associated with a more unstable atmospheric boundary layer, and increased evaporation and potential for convective activity. This response is basin-wide in character, as manifested by the Caribbean rainfall anomalies described below.

Table 2 summarizes the  $W^*$  values of the Wilcoxon two-sample sum statistic for the GHCN index during 1949-1999 (section 2) as a function of phase of ENSO (warm or cold) and of the NAO (positive or negative). During JAS(0), the 95% significance level is reached when all warm ENSO events ( $n = 11$ ) are compared to neutral seasons ( $m = 30$ ), meaning that a warm ENSO event is associated with below average rainfall in the Caribbean. It is also reached when only the warm ENSO events preceded by the positive NAO phase (7 out of the 11 cases) are compared to the neutral composite. In these cases, the ENSO and NAO impacts combine to make the negative rainfall anomalies even larger. The reverse case of cold ENSO and negative NAO (3 out of 10), when the phenomena should combine to give positive rainfall anomalies in JAS(0), also stands out as highly significant. Conversely, the 95% significance level is far from being reached in the case of warm ENSO and negative NAO (4 out of 11 cases), and in the case of cold ENSO and positive NAO (7 out of 10 cases). When the two phenomena have competing effects on Caribbean rainfall these seasons cannot be distinguished from neutral conditions.



During AMJ(+1), rainfall anomalies in the Caribbean are significantly different from neutral only when ENSO and the NAO interfere constructively: warm ENSO – negative NAO (5 out of 11 cases), cold ENSO – positive NAO (3 out of 10 cases). It is interesting to note that when the sign of the NAO only is taken into consideration, regardless of phase of ENSO, the effect of the NAO on Caribbean rainfall is found to be significant in spring only. When the Wilcoxon two-sample sum statistic is applied to the comparison of the 21 years of negative NAO with the 30 years of positive NAO, then the rainfall difference between the two phases of the NAO is significant at the 95% level only in spring, not significant in summer (see table 2).

Thus the picture of the interaction between ENSO and NAO effects on Caribbean rainfall is dynamically consistent and also statistically significant. To explain the change in the ENSO teleconnection to the Caribbean basin expressed by the Xie-Arkin data, we first note that 4 out of 6 of the last El Niños have been preceded by a positive NAO (fig. 6, left panel). The effect on Caribbean rainfall during JAS(0) is clearly displayed in figure 9. Comparing fig. 9 to fig. 5 (top left panel), we see that the dry anomalies that cover the Caribbean, Central America and the tropical North Atlantic in JAS(0) are enhanced during the 4 events, as expected given the nefarious combination of a warm ENSO and a positive NAO. In AMJ(+1), 5 out of 6 warm ENSO events in the last 20 years have coincided with a positive NAO. As we have seen, those phases of the two phenomena have opposing effects on Caribbean rainfall. We suggest that this opposition accounts for the disappearance of the positive rainfall anomaly expected from ENSO. At the same time, the fact that 2 out of 3 cold events also have coincided with a positive NAO phase is manifest in the significant negative tropical North Atlantic rainfall anomalies of fig. 5 (bottom right panel). Therefore, the apparently unusual ENSO teleconnection to Caribbean

rainfall over the last 20 years can be interpreted in a manner consistent with the longer record, but only if the role of the North Atlantic is included in the picture. The persistent positive phase of the NAO, combined with ENSO, accounts for the variations observed in the Xie-Arkin satellite dataset.

## 5. The interaction between the NAO and ENSO during winter

In the present section, we briefly digress from Caribbean rainfall variability to focus on the relationship between the Southern Oscillation (SO) and the North Atlantic Oscillation. In view of their combined impact on Caribbean rainfall, we are specifically interested in understanding their interaction in the subtropical North Atlantic. We focus on the winter season (January to March), because it is the time when the NAO manifests greatest variability, explaining a large portion of the variance of the wintertime extratropical climate. It is also the time when ENSO reaches its peak intensity in the central equatorial Pacific (Rasmusson and Carpenter 1982), and the ENSO-related wave train to extratropical latitudes manifests itself in the form of the Pacific-North American (PNA) teleconnection pattern.

Warm ENSO composites of wintertime mean SLP and surface temperature during the NCEP-NCAR reanalysis period are presented in figure 10. The PNA is in its positive phase, prevalent during warm ENSO events. The low pressure centers associated with this pattern are evident in fig. 10 (top left panel), off the northwest and southeast coasts of North America. These anomalies are statistically significant at the 95% level. The tropical Pacific high pressure region is just off the map, its center positioned between 10°N and 20°N west of the dateline. The high latitude high pressure center is not statistically significant at the 95% level. The change in

the meridional gradient in the North Atlantic is of the same sign as would be associated with a negative phase of the NAO, but it is not spatially in phase with the NAO pattern. Rather, its centers of action are shifted westward by approximately  $30^\circ$ . Surface temperature is warmer than average in a latitudinal band across the North American continent between  $40^\circ\text{N}$  and  $60^\circ\text{N}$ , and cooler at lower latitudes, particularly over the Gulf of Mexico region (fig. 10, top right panel).

When the NAO-dependent component of the signal is subtracted by means of a least-squares regression onto its December-March index (Hurrell 1995), and the same warm ENSO composites are drawn again, the result is an increase in the statistical significance of the SLP response to the ENSO teleconnection in the western North Atlantic, especially at high latitudes (fig. 10, bottom left panel). The surface temperature signal over North America persists, reaching the 95% statistical significance level over northeastern Canada (fig. 10, bottom right panel). This is consistent with the interpretation that the NAO has partially masked the impact of ENSO on North Atlantic SLP and on surface temperature over eastern North America during the recent period.

A warm ENSO event favored low pressure anomalies over the subtropical North Atlantic and high pressure anomalies over the high latitude North Atlantic, i.e. a negative-NAO-like pattern in SLP, but it did not increase the frequency of occurrence of a negative NAO. Warm ENSO and positive NAO, associated with SLP anomalies of opposite sign in the North Atlantic, have coexisted over the last 20 years. If anything, the two patterns have ended up masking each other. The surface temperature anomalies over northeastern Canada are an example of such a superposition, since they would tend to be positive during a warm ENSO event, and negative during the positive phase of the NAO, and are not statistically significant when the two signals

are not separated.

Even without data from the recent period, Rogers (1984) also concluded that the two oscillations are not related. This conclusion was reached despite significant coherence in the spectra of the NAO and SO indices at 5-6 years period, because too many instances were noted in which the predicted phase relationship between the two patterns was not verified. The more recurrent phase relationship, of a warm ENSO-negative NAO association, or low/wet SO-Atlantic blocking association, in the terminology of Rogers (1984), is reversed in Huang et al. (1998). Huang et al. (1998) instead capture the association between warm ENSO and positive NAO that is characteristic of the early part of the century and of the more recent period, but not of the 1940-1980 period (fig. 6, right panel). Therefore, we would caution that the interpretation of their peak in the coherence spectrum at 5.7 years period in terms of a more stringent relationship between strong ENSO events and the positive phase of the NAO is ultimately dependent on the trends in the NAO, recent and past, rather than on a proven dynamical mechanism.

## 6. Discussion and Conclusions

We started this investigation with a comparison of the ENSO teleconnection to the Caribbean and Central America as depicted by two independent datasets. The Xie-Arkin (1996, 1997) rainfall dataset, a recent compilation of satellite proxies and rain gauge measurements, was compared with results from our previous study into the causes of the interannual variability of Caribbean rainfall (GKC), which relied on a large set of land station data collected during an earlier period. In this region the rain gauge data is much more limited for the past 20 years, and the satellite proxies are essential to obtain a complete picture of the variability. We found that the dry signal

which precedes peak ENSO conditions, during the summer of year (0), is consistently present in the recent 20-year satellite record. However, rainfall anomalies following warm ENSO events during the most recent 20 years do not display the wet signal expected during spring (Chen et al. 1997), also associated with the delayed warming of the tropical North Atlantic (Enfield and Mayer 1997).

These findings prompted research into the possible explanations for such an incongruence. Since North Atlantic climate is the other well-known large-scale player affecting Caribbean rainfall variability, we directed our efforts towards that sector. The timing within the annual cycle of the change in the ENSO teleconnection coincides with the season of greatest influence of North Atlantic SLP and SST on the region. A higher than average wintertime North Atlantic High, or equivalently, a positive NAO index, is associated with stronger trades, hence higher than average heat flux from the ocean to the atmosphere at tropical latitudes. This acts to cool the surface of the tropical ocean, affecting deep convection at the start of the rainy season in spring. (Signs in the anomalies are reversed in the case of a lower than average North Atlantic High.) The overall negative trend in Caribbean spring rainfall during the last 20 years (fig. 4, right panel) is consistent with the concurrent positive trend in the NAO index. With regards to the ENSO-NAO interaction, we note that the NAO was in its negative phase during the winter immediately preceding AMJ(+1) in 4 out of 5 warm ENSO events during 1949-1979, whereas in 5 out of 6 warm ENSO events since 1979 it has been in its positive phase. We explain the recent disappearance of the springtime ENSO teleconnection in terms of a linear superposition of effects. In the past 20 years, the delayed warming of the tropical North Atlantic, normally associated with a warm ENSO event, has been counteracted by the cooling associated with a

stronger than average NAO, resulting in cancellation of the effects. Similarly, in the summer-time, the warm ENSO signal of drier than average conditions in the Caribbean is enhanced when winter of year (0) witnesses a positive NAO phase, as has happened in 7 out of 11 warm ENSO events during the past 50 years.

We claim that the change noted in ENSO's influence on the Caribbean basin during the last 20 years is related to changes in the North Atlantic sector. What appears to be at first glance a non-stationarity of the ENSO teleconnection to the Caribbean on the interdecadal time scale, with decades characterized by a strong ENSO signal (the 1950s, 1960s and 1970s), and decades of vanishing impact (the 1980s and 1990s), can be largely explained in terms of the interaction of the independent impacts of the NAO and ENSO on Caribbean climate. This agrees well with the work of van Loon and Madden (1981) on the variability of the impact of ENSO on North Atlantic climate. They, too, observed that the link between the Southern Oscillation and North Atlantic SLP was stronger during the 1960s and 1970s, and weaker during the earlier part of the century, noting that the NAO can at times be in phase, at other times out of phase with ENSO. ENSO and the NAO appear to be independent manifestations of climate variability, even though their influence overlaps in the North Atlantic region, because:

- spatially, their centers of action in the North Atlantic are not coincident: ENSO-related SLP anomalies are shifted westward by about  $30^\circ$  with respect to the centers of action of the NAO.
- temporally, the correlation between any two indices representing the two phenomena is not significant. No consistent relationship is evident from the analysis of fig. 6 (right panel),

which spans the entire 20<sup>th</sup> century. For example, a warm ENSO is more frequently associated with a positive NAO during the earlier and later parts of the last century, and with a negative NAO during the intervening period. The positive NAO phase occurs with ENSO events of either sign during the recent decades.

The recent disappearance of the springtime ENSO teleconnection to the Caribbean is consistent with the observation that rainfall in 12 stations in Puerto Rico has been significantly below average during this past decade (Larsen 1999). If ENSO and the NAO are independent, then one does not need to explain the coincidence of the warm ENSO events of the 1980s and 1990s with the predominant positive phase of the NAO. While this hypothesis seems well supported by our diagnostic study, other causes cannot be ruled out, and should be considered in, for example, well designed numerical modeling studies.

Variability internal to the ENSO system, which has been related to a shift in the background climate in the North Pacific (Trenberth 1990; Wang 1995), in the direction of the warm phase of the ENSO-like decadal mode of variability (Zhang et al 1997; Gerreaud and Battisti 1999), could affect the ENSO teleconnection. This could occur through a shift in the location of the centers of deep convection, as postulated by Kumar et al. (1999). For example, the superposition of the warm phase of the decadal ENSO-like mode with the decay phase of a warm event could result in a warmer than average central and eastern equatorial Pacific during spring of year (+1). The anomalously warm central and eastern equatorial Pacific waters could in turn still be capable of driving anomalous deep convection, altering the balance between the remotely-forced atmospheric component of the ENSO teleconnection to the Caribbean, and the local, tropical

North Atlantic SST response. In the Caribbean, the local response of wet conditions locally forced by warm SST anomalies could be contrasted by surface divergence remotely forced from the Pacific. This situation also is consistent with the absence of a clear wet anomaly following the more recent warm ENSO events. What remains to be explained is whether the observed Pacific and Atlantic 'regime shifts' are a part of natural climate variability, or the response of the climate system to the anthropogenic increase in greenhouse gases.

*Acknowledgments.* This work was supported by the U.S. National Oceanic and Atmospheric Administration under grant NA86GP0515. We wish to thank John Chiang, Alexey Kaplan, Balaji Rajagopalan, Richard Seager, Steve Zebiak, Ping Chang and David Enfield for the time dedicated to discussions, and the anonymous reviewers for helpful comments.



## References

- Akaike, H., 1974: A new look at the statistical model identification. *IEEE Trans. Autom. Control*, **AC-19**, 716–723.
- Alfaro, E. and Enfield, D. B., 1999: The rainy season in Central America: an initial success in prediction. *IAI NewsLetter*, **20**, 20–22.
- Barnston, A. and Livezey, R. E., 1987: Classification, seasonality and persistence of low-frequency atmospheric circulation patterns. *Mon. Wea. Rev.*, **115**, 1083–1126.
- Cayan, D. R., 1992: Latent and sensible heat flux anomalies over the northern oceans: the connection to monthly atmospheric circulation. *J. Climate*, **5**, 354–369.
- Chen, A., Roy, A., McTavish, J., Taylor, M., and Marx, L., 1997: Using SST anomalies to predict flood and drought conditions for the Caribbean. *COLA Rep.*, **49**. Available from the Center for Land-Ocean-Atmosphere Studies, 4041 Powder Mill Road, Suite 302, Calverton, MD 20705-3106, U.S.A.
- Chiang, J. C. H., Kushnir, Y., and Zebiak, S. E., 2000: Interdecadal changes in eastern Pacific ITCZ variability and its influence on the Atlantic ITCZ. *Geophys. Res. Lett.* in press.
- Cook, E. R., Meko, D. M., Stahle, D. W., and Cleaveland, M. K., 1996: Tree-ring reconstructions of past drought across the conterminous United States: tests of a regression method and calibration/verification results. *Tree Rings, Environment and Humanity*, pp. 155–169. Dean, J. S., D. M. Meko and T. W. Swetnam, Eds., Radiocarbon.
- Cook, E. R., Meko, D. M., Stahle, D. W., and Cleaveland, M. K., 1999: Drought reconstructions for the continental United States. *J. Climate*, **12**, 1145–1162.
- Covey, D. L. and Hastenrath, S., 1978: Pacific El Niño phenomenon and the Atlantic circulation. *Mon. Wea. Rev.*, **106**, 1280–1287.
- Curtis, S. and Hastenrath, S., 1995: Forcing of anomalous sea surface temperature evolution in the tropical Atlantic during Pacific warm events. *J. Geophys. Res.*, **100**, 15835–15847.

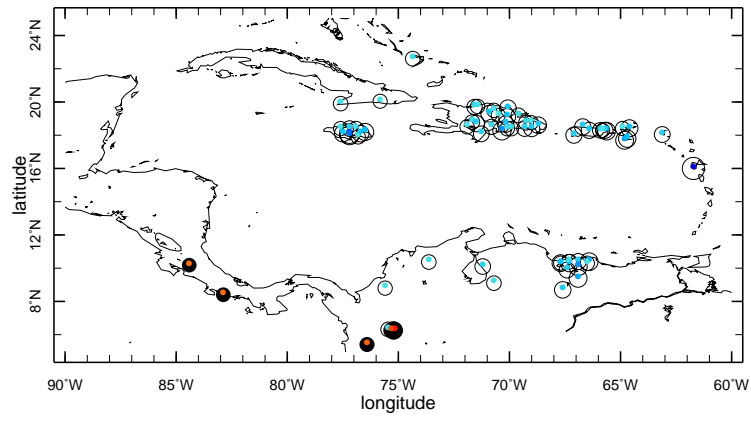
- Dai, A., Fung, I. Y., and Del Genio, A. D., 1997: Surface observed global land precipitation variations during 1900-88. *J. Climate*, **11**, 2943–2962.
- Enfield, D. B., 1996: Relationship of inter-American rainfall to tropical Atlantic and Pacific SST variability. *Geophys. Res. Lett.*, **23**, 3305–3308.
- Enfield, D. B. and Alfaro, E. J., 1999: The dependence of Caribbean rainfall on the interaction of the tropical Atlantic and Pacific Oceans. *J. Climate*, **12**, 2093–2103.
- Enfield, D. B. and Mayer, D. A., 1997: Tropical Atlantic sea surface temperature variability and its relation to El Niño-Southern Oscillation. *J. Geophys. Res.*, **102**, 929–945.
- Gerreaud, R. D. and Battisti, D. S., 1999: Interannual (ENSO) and interdecadal (ENSO-like) variability in the Southern Hemisphere tropospheric circulation. *J. Climate*, **12**, 2113–2123.
- Giannini, A., Kushnir, Y., and Cane, M. A., 2000: Interannual variability of Caribbean rainfall, ENSO and the Atlantic Ocean. *J. Climate*, **13**, 297–311.
- Hastenrath, S., 1976: Variations in low-latitude circulation and extreme climatic events in the tropical Americas. *J. Atmos. Sci.*, **33**, 202–215.
- Hastenrath, S., 1984: Interannual variability and annual cycle: mechanisms of circulation and climate in the tropical Atlantic sector. *Mon. Wea. Rev.*, **112**, 1097–1107.
- Hastenrath, S. and Heller, L., 1977: Dynamics of climatic hazards in northeast Brazil. *Q. J. R. Meteor. Soc.*, **103**, 77–92.
- Hollander, M. and Wolfe, D. A., 1999: Nonparametric statistical methods. Wiley-Interscience, John Wiley and Sons, INC.
- Horel, J. D. and Wallace, J. M., 1981: Planetary scale atmospheric phenomena associated with the Southern Oscillation. *Mon. Wea. Rev.*, **109**, 813–829.
- Huang, J., Higuchi, K., and Shabbar, A., 1998: The relationship between the North Atlantic Oscillation and the El Niño-Southern Oscillation. *Geophys. Res. Lett.*, **25(14)**, 2707–2710.

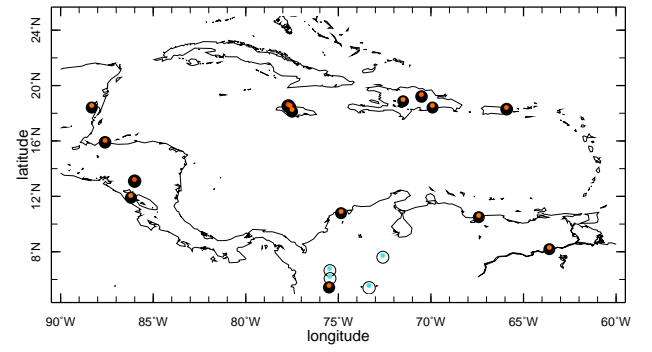
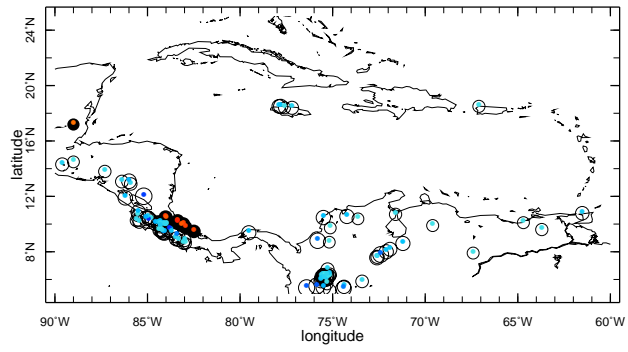
- Hulme, M., 1992: A 1951-80 global land precipitation climatology for the evaluation of general circulation models. *Clim. Dyn.*, **7**, 57–72.
- Hurrell, J. W., 1995: Decadal trends in the North Atlantic Oscillation regional temperatures and precipitation. *Science*, **269**, 676–679.
- Kalnay, E. and Coauthors, 1996: The NCEP-NCAR 40-year reanalysis project. *Bull. Amer. Meteor. Soc.*, **77**, 437–471.
- Kaplan, A., Cane, M. A., Kushnir, Y., Clement, A. C., Blumenthal, M. B., and Rajagopalan, B., 1998: Analyses of global sea surface temperature 1856-1991. *J. Geophys. Res.*, **103**, 18,567–18,589.
- Kaplan, A., Kushnir, Y., Cane, M. A., and Blumenthal, M. B., 1997: Reduced space optimal analysis for historical datasets: 136 years of Atlantic sea surface temperatures. *J. Geophys. Res.*, **102**, 27,835–27,860.
- Kiladis, G. N. and Diaz, H. F., 1989: Global climatic anomalies associated with extremes in the Southern Oscillation. *J. Climate*, **2**, 1069–1090.
- Knaff, J. A., 1997: Implications of summertime sea level pressure anomalies in the tropical Atlantic region. *J. Climate*, **10**, 789–804.
- Krishna Kumar, K., Rajagopalan, B., and Cane, M. A., 1999: On the weakening relationship between the Indian monsoon and ENSO. *Science*, **284**, 2165–2159.
- Larsen, M. C., 1999: Rainfall, drought, and water resources in the Northeastern Caribbean. *Phys. Geography*. submitted.
- Lau, N.-C., 1997: Interactions between global SST anomalies and the midlatitude atmospheric circulation. *Bull. Amer. Meteor. Soc.*, **78**, 21–33.
- Lau, N.-C. and Nath, M. J., 1994: A modeling study of the relative roles of tropical and extratropical sst anomalies in the variability of the global atmosphere-ocean system. *J. Climate*, **7**, 1184–1207.

- Lau, N.-C. and Nath, M. J., 1996: The role of the 'atmospheric bridge' in linking tropical Pacific ENSO events to extratropical SST anomalies. *J. Climate*, **9**, 2036–2057.
- Nobre, P. and Shukla, J., 1996: Variations of sea surface temperature, wind stress, and rainfall over the tropical Atlantic and South America. *J. Climate*, **9**, 2464–2479.
- Pan, Y. H. and Oort, A. H., 1983: Global climate variations connected with sea surface temperature anomalies in the eastern equatorial Pacific Ocean for the 1958-73 period. *Mon. Wea. Rev.*, **111**, 1244–1258.
- Poveda, G. and Mesa, O. J., 1997: Feedbacks between hydrological processes in tropical South America and large-scale ocean-atmospheric phenomena. *J. Climate*, **10**, 2690–2702.
- Rasmusson, E. M. and Carpenter, T. H., 1982: Variations in tropical sea surface temperature and surface wind fields associated with the Southern Oscillation/El Niño. *Mon. Wea. Rev.*, **110**, 354–384.
- Rogers, J. C., 1984: The association between the North Atlantic Oscillation and the Southern Oscillation in the Northern Hemisphere. *Mon. Wea. Rev.*, **112**, 1999–2015.
- Ropelewski, C. F. and Halpert, M. S., 1987: Global and regional precipitation patterns associated with the El Niño/Southern Oscillation. *Mon. Wea. Rev.*, **115**, 1606–1626.
- Ropelewski, C. F. and Halpert, M. S., 1996: Quantifying Southern Oscillation-precipitation relationships. *J. Climate*, **9**, 1043–1059.
- Schultz, D. M., Bracken, W. E., and Bosart, L. F., 1998: Planetary- and synoptic-scale signatures associated with Central American cold surges. *Mon. Wea. Rev.*, **126**, 5–27.
- Seager, R., Kushnir, Y., Visbeck, M., Naik, N., Miller, J., Krahnmann, G., and Cullen, H., 2000: Causes of Atlantic Ocean climate variability between 1958 and 1998. *J. Climate*, **13**, 2845–2862.
- Snedecor, G. W. and Cochran, W. G., 1989: Statistical methods, 8th edition. Iowa State University Press, Ames, Iowa, 503 pp.

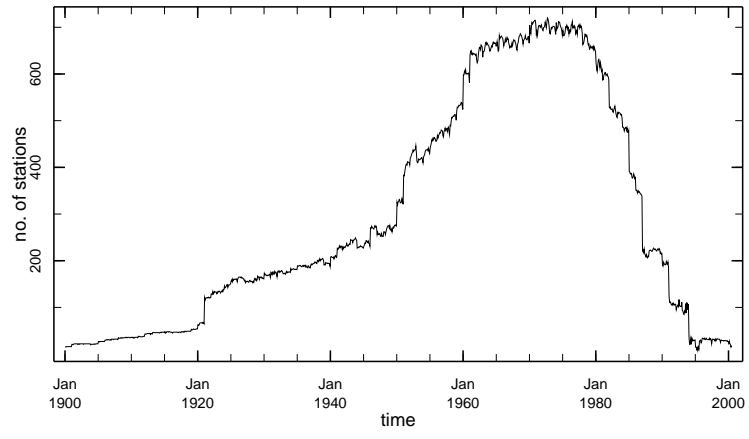
- Trenberth, K. E., 1990: Recent observed interdecadal climate changes in the Northern Hemisphere. *Bull. Amer. Meteor. Soc.*, **71**, 988–993.
- Trenberth, K. E., Branstator, G. W., Karoly, D., Kumar, A., Lau, N.-C., and Ropelewski, C. F., 1998: Progress during TOGA in understanding and modeling global teleconnections associated with tropical sea surface temperatures. *J. Geophys. Res.*, **103**, 14291–14324.
- van Loon, H. and Madden, R. A., 1981: The Southern Oscillation. Part I: global associations with pressure and temperature in northern winter. *Mon. Wea. Rev.*, **109**, 1150–1162.
- van Loon, H. and Rogers, J. C., 1978: Seesaw in winter temperatures between Greenland and northern Europe Part I: general description. *Mon. Wea. Rev.*, **106**, 296–310.
- Vose, R. S., Schmoyer, R. L., Steurer, P. M., Peterson, T. C., Heim, R., Karl, T. R., and Eischeid, J., 1992: The Global Historical Climatology Network: long-term monthly temperature, precipitation, sea level pressure, and station pressure data. ORNL/CDIAC-53, NDP-041. Carbon Dioxide Information Analysis Center, Oak Ridge National Laboratory, Oak Ridge, Tennessee.
- Wallace, J. M. and Gutzler, D. S., 1981: Teleconnections in the geopotential height field during the northern hemisphere winter. *Mon. Wea. Rev.*, **109**, 784–812.
- Wang, B., 1995: Interdecadal changes in El Niño onset in the last four decades. *J. Climate*, **8**, 267–285.
- Waylen, P. R., Caviedes, C. N., and Quesada, M. E., 1996: Interannual variability of monthly precipitation in Costa Rica. *J. Climate*, **9**, 2606–2613.
- Xie, P. and Arkin, P. A., 1996: Analyses of global monthly precipitation using gauge observations, satellite estimates, and numerical model predictions. *J. Climate*, **9**, 840–858.
- Xie, P. and Arkin, P. A., 1997: Global precipitation: A 17-year monthly analysis based on gauge observations, satellite estimates and numerical model outputs. *Bull. Amer. Meteor. Soc.*, **78**, 2539–2558.

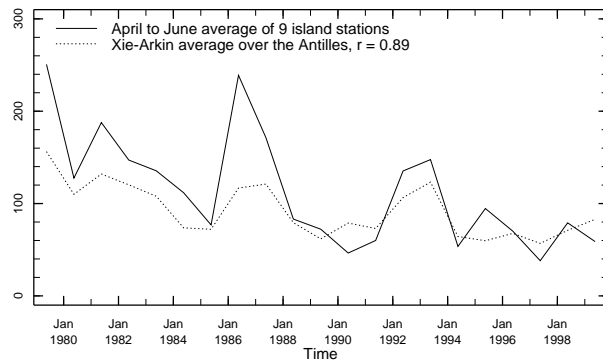
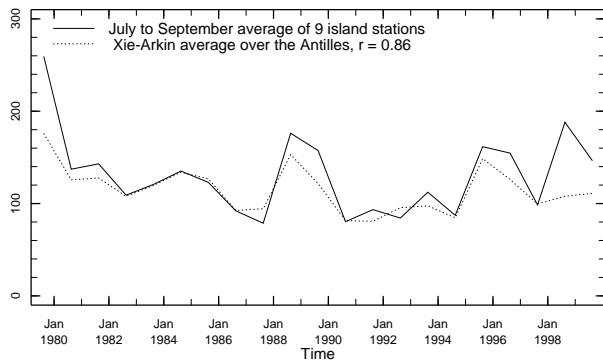
Zhang, Y., Wallace, J. M., and Battisti, D. S., 1997: ENSO-like interdecadal variability: 1900-93.  
*J. Climate*, **10**, 1004–1020.

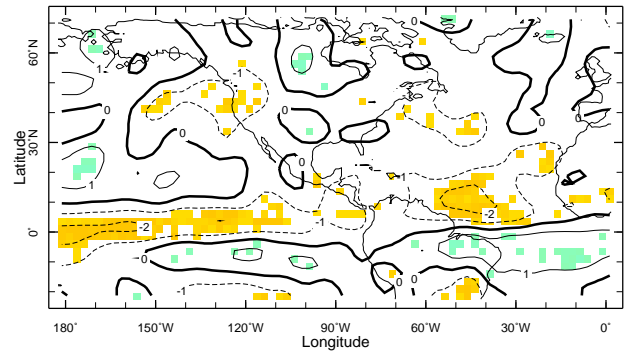
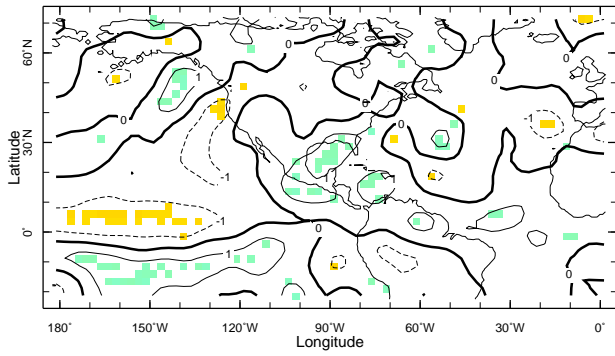
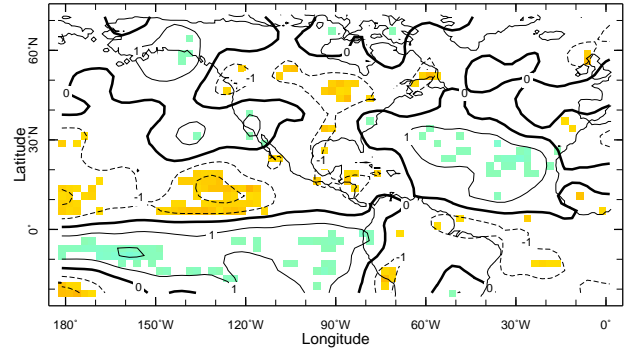
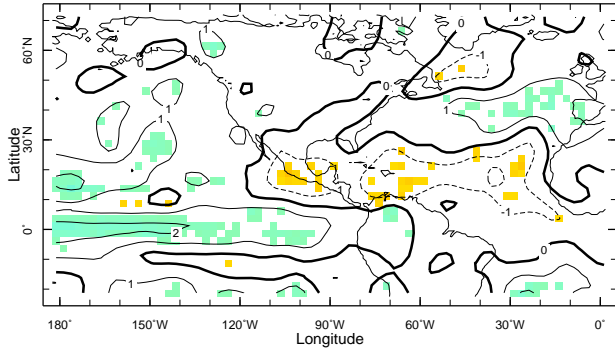


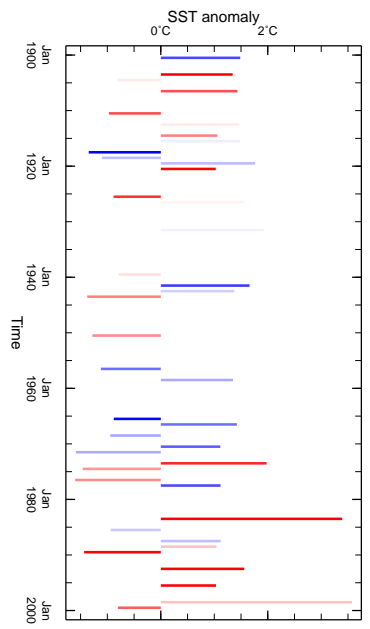
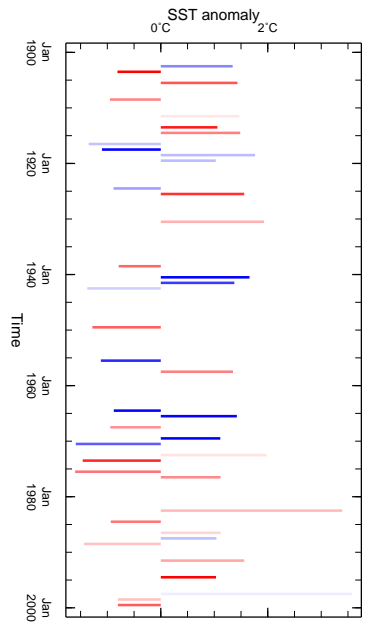


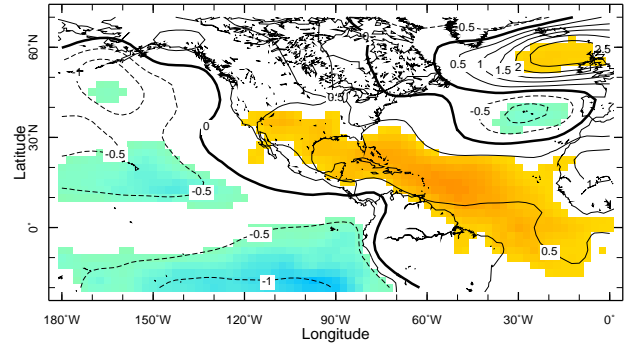
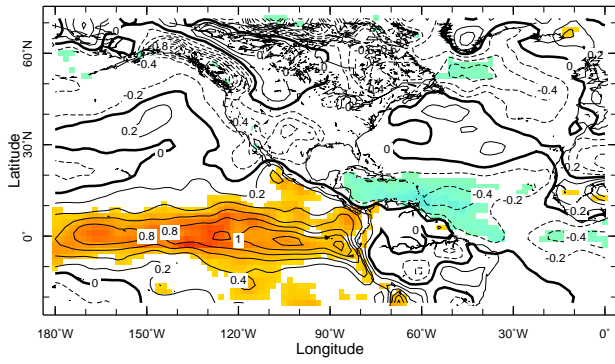
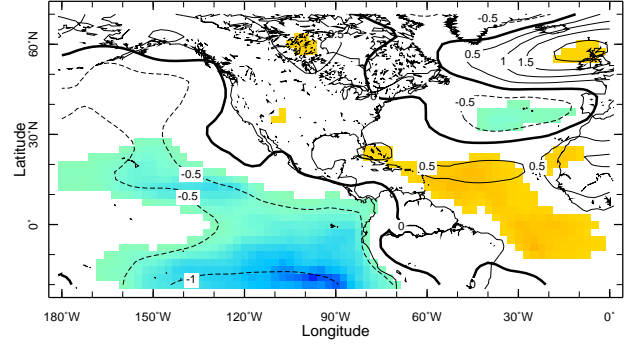
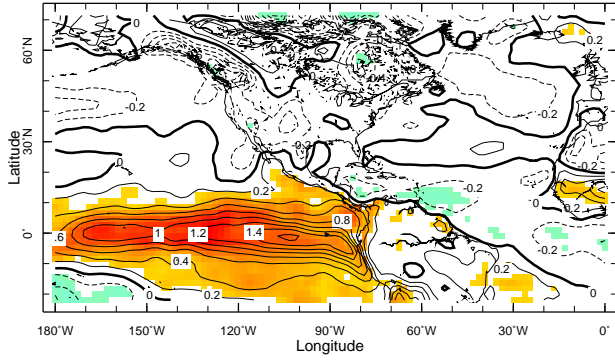


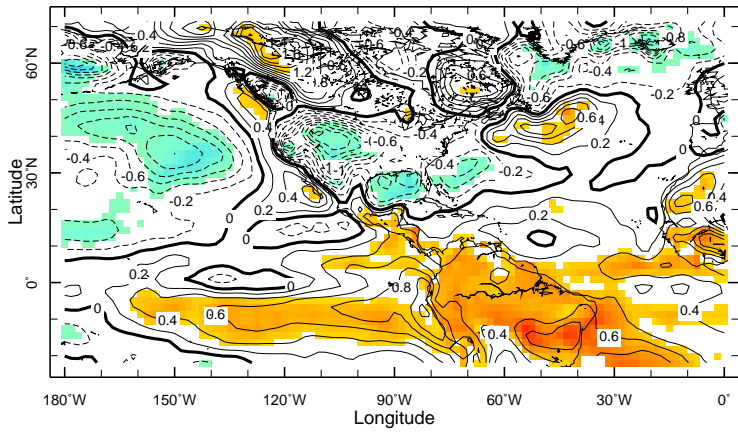
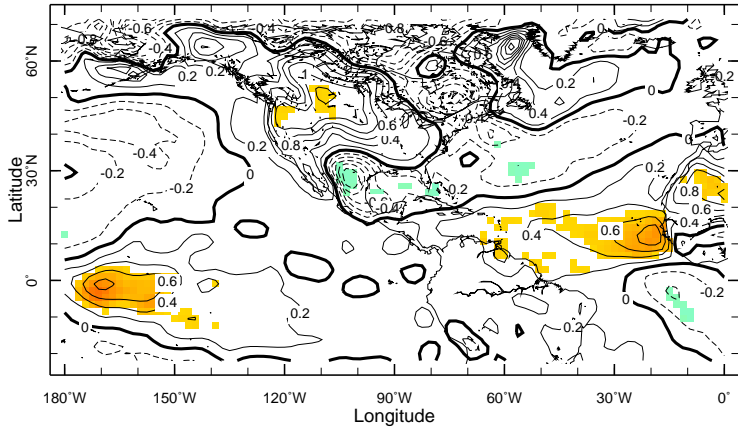
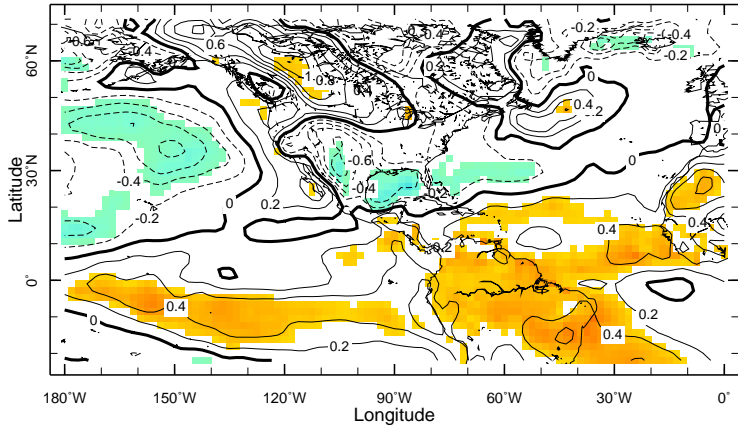


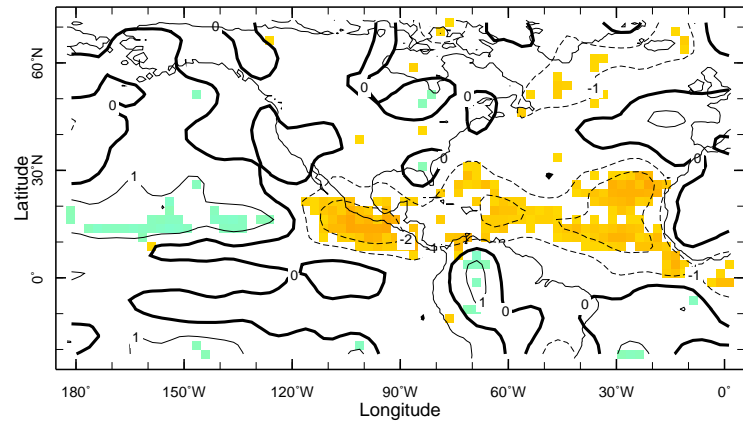












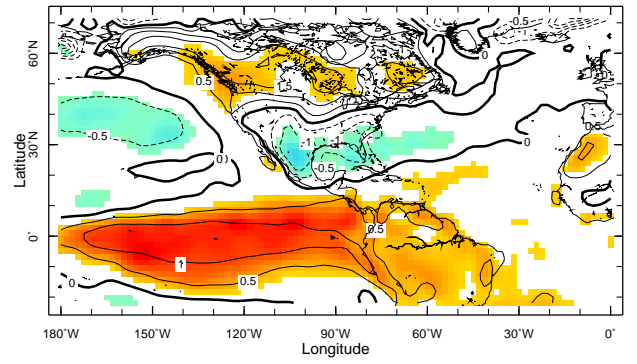
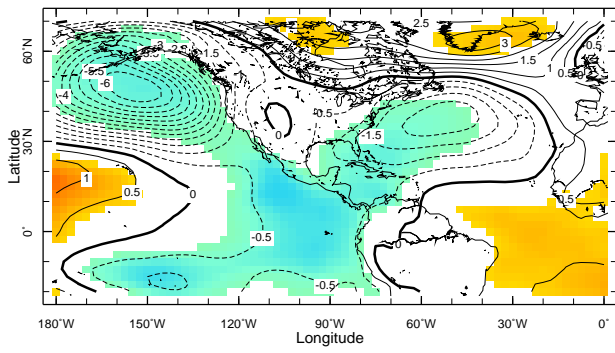
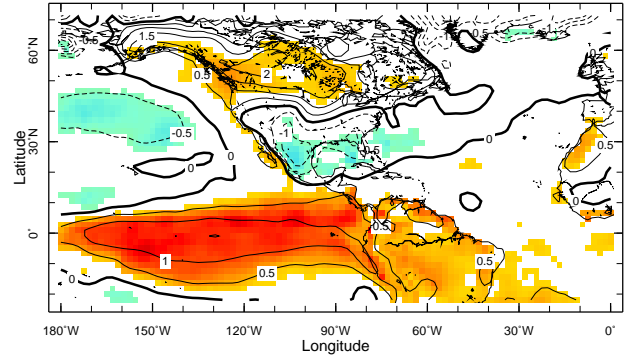
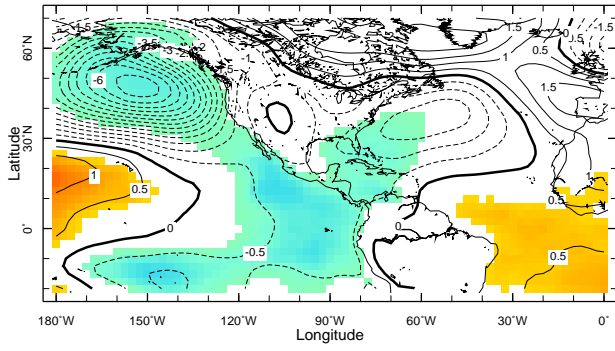




## Figure Captions

Figure 1. Correlation of the December-March NAO index with station rainfall during the following April-June, 1949-1980. Only those stations that have at least 66% of the data and reach a statistically significant correlation value of 0.425 (95% confidence level for  $\nu = 20$ ) are plotted. Full (open) circles with a red (blue) center indicate positive (negative) correlation.

Figure 2. Correlation of the December(0)-January(+1) Niño-3 index with station rainfall: (left) during July-September (0); (right) during April-June (+1), 1949-1980. Only those stations that have at least 66% of the data and reach a statistically significant correlation value of 0.425 (95% confidence level for  $\nu = 20$ ) are plotted. Full (open) circles with a red (blue) center indicate positive (negative) correlation.

Figure 3. The number of weather stations recording monthly rainfall in the Caribbean and Central America ( $5^{\circ}\text{N}$ ,  $25^{\circ}\text{N}$ ;  $90^{\circ}\text{W}$ ,  $60^{\circ}\text{W}$ ) during the 20<sup>th</sup> century. From the Global Historical Climatology Network.

Figure 4. Comparison of the interannual variability of rainfall over the Antilles Islands as depicted by an index of 9 GHCN stations (solid line), and by the Xie-Arkin dataset averaged between  $15$  and  $22.5^{\circ}\text{N}$ ,  $80$  and  $60^{\circ}\text{W}$  (dashed line). (left) Summer,  $r = 0.86$ ; (right) spring,  $r = 0.89$ .

Figure 5. Ranked rainfall anomalies during ENSO events in the Xie-Arkin dataset (1979-1999). *Top row*: warm events. (left) July-September (0), (right) April-June (+1). *Bottom row*: cold events. (left) July-September (0), (right) April-June (+1). Contours are in units of standard deviation. Shading indicates statistical significance of the ranked anomalies at the 95% confidence level.

Figure 6. Time series of the December(0)-January(+1) Niño-3, colored by the magnitude of the December-to-March NAO index. The height of the bar represents the value of Niño-3, the color intensity represents the value of the NAO index, red for positive, blue for negative values. (left) Niño-3 colored by the previous winter NAO index, with both indices affecting the JAS(0) season. (right) Niño-3 colored by the simultaneous NAO index, with both indices affecting the AMJ(+1) season.

Figure 7. NCEP-NCAR Reanalysis (1949-1999). Warm ENSO composites of surface temperature and

mean sea level pressure during the JAS(0) season. *Top row*: composites for all 11 events, temperature (left), and pressure (right). *Bottom row*: events when the NAO index during the preceding winter is positive (7 out of 11 cases) (left) temperature, (right) pressure. Contours are  $0.2^{\circ}\text{C}$ ,  $0.5\text{ hPa}$ . Shading indicates statistical significance of the anomalies at the 95% confidence level.

Figure 8. NCEP-NCAR Reanalysis (1949-1999). Warm ENSO composites of surface temperature during the AMJ(+1) season. *Top*: all 11 warm ENSO events. *Middle*: events when the NAO index during the preceding winter is negative (5 out of 11 cases). *Bottom*: events when the NAO index during the preceding winter is positive (the remaining 6 out of 11 cases). Contours are  $0.2^{\circ}\text{C}$ . Shading indicates statistical significance of the anomalies at the 95% confidence level.

Figure 9. Xie-Arkin precipitation (1979-1999). Warm ENSO composite of ranked precipitation during the JAS(0) season, when the NAO during the preceding winter is positive (4 out of 6 cases). Contours are in units of standard deviation. Shading indicates statistical significance of the ranked anomalies at the 95% confidence level.

Figure 10. NCEP-NCAR Reanalysis (1949-1999). Warm ENSO composites of mean sea level pressure and surface temperature during the JFM(+1) season, (left) pressure, (right) temperature. In the *bottom row*, the NAO signal has been subtracted by means of linear regression, (left) pressure, (right) temperature. Contours are  $0.5\text{ hPa}$ ,  $0.5^{\circ}\text{C}$ . Shading indicates statistical significance of the anomalies at the 95% confidence level.

	a	b	c	r	AIC
Kaplan SST (1900-91)	0.03	-0.31	-	0.31	-3.0
	-0.04	-	0.45	0.43	-12.7
	-0.01	-0.29	0.44	0.52	-20.5
NCEP sfc temp (1949-99)	0.03	-0.26	-	0.26	2.8
	-0.05	-	0.54	0.60	-15.8
	-0.02	-0.32	0.56	0.67	-22.0
NCEP sfc temp (1979-1999)	0.14	-0.23	-	0.23	6.3
	-0.16	-	0.44	0.56	-0.4
	0.02	-0.31	0.47	0.64	-0.4

	JAS(0)			AMJ(+1)		
	warm ENSO	cold ENSO	all years	warm ENSO	cold ENSO	all years
All ENSO events	<b>-2.94</b> (11)	1.09 (10)	–	0.59 (11)	-1.56 (10)	–
positive NAO	<b>-3.30</b> (7)	-0.27 (7)	– (30)	-1.52 (6)	<b>-3.06</b> (3)	– (30)
negative NAO	0.78 (4)	<b>3.99</b> (3)	0.67 (21)	<b>1.99</b> (5)	-0.47 (7)	<b>2.12</b> (21)

## Table Captions

Table 1. Results of the regression of an index of springtime tropical North Atlantic SST (tNA) against Niño-3 and the NAO: a, b and c are the regression coefficients associated with the constant, NAO and Niño-3 respectively;  $r$  is the correlation coefficient between observed and modeled tNA, and AIC is the Akaike information criterion. See text for details.

Table 2. The  $W^*$  parameter in the Wilcoxon two-sample sum statistic for the GHCN index of Caribbean rainfall, JAS(0) and AMJ(+1) seasons during 1949-1999. Values statistically significant at the 95% level (1.96 standard deviations) are in bold type.